TEVATRON SEARCHES FOR BSM BROUT-ENGLERT-HIGGS BOSONS

A. Kasmi
Department of Physics, Baylor University, One Bear Place 97316, Waco, TX, U.S.A

Using the full dataset delivered by the Fermilab Tevatron, the CDF and D0 experiments are actively seeking evidence for the Brout-Englert-Higgs (BEH) boson in beyond-the-standard-model (BSM) scenarios, particularly in supersymmetric models and fermiophobic scenarios. The simplest supersymmetric extension to the standard model, the Minimal Supersymmetric Standard Model (MSSM), requires the introduction of two Higgs doublet fields, which predict the existence of five physical BEH bosons after symmetry breaking. Alternatively, in fermiophobic models, the symmetry breaking mechanism responsible for giving masses to gauge bosons is separate from that which generates the fermion masses. A selection of final results from searches for the BSM BEH boson carried out by CDF and D0 is presented.

1 Introduction

The SM of particle physics has proven to be a robust theoretical model that very accurately describes the properties of elementary particles and the forces of interaction between them. However, the origin of mass is still an unsolved mystery. The theory suggests that particles acquire mass due to electroweak interactions with the Higgs boson via electroweak symmetry breaking.[1] In the SM, the spontaneous symmetry breaking mechanism requires a single doublet of a complex scalar field. However, it is likely that nature does not follow this minimal version and that a multi-Higgs sector may be required. In this note, we describe two models that require a doublet Higgs field: fermiophobic Higgs models[2] and MSSM.[3]

1.1 Fermiophobic Model

In fermiophobic models scenario, the symmetry breaking mechanism responsible for giving Higgs masses to gauge bosons is separate from that which generates the fermion masses. In the benchmark model considered, a fermiophobic Higgs boson (H_f) assumes SM couplings to bosons and vanishing couplings to all fermions. The gluon fusion process is then suppressed and only VH

and VBF processes remain as shown in Fig. 1 (a and b). Hence, a reduction in the cross section by a factor of 4 is predicted. However, this reduction is compensated by the high diphoton branching fraction for this model. Direct searches at LEP set a lower limit on the fermiophobic Higgs boson mass of 109.7 GeV with 95% C.L[4]. We present a search for the fermiophobic Higgs boson in the diphoton final state using 10 fb^{-1} of data for both the D0 and CDF experiments collected from $p\bar{p}$ collisions at $\sqrt{s} = 1.96$ TeV from the Fermilab Tevatron Collider.

1.2 MSSM Model

As an extension to the SM, Supersymmetry (SUSY) provides a natural solution to the hierarchy problem, a dark matter candidate, and GUT-scale unification. The MSSM predicts the existence of five physical Higgs bosons after symmetry breaking. Three of these are neutral (h, H, and A) and two are charged $H^{\pm}$. The ratio of the vacuum expectation values of the two doublets is denoted by $\tan\beta$. At leading order the Higgs sector can be described by two parameters chosen here to be M_A (the mass of the A) and $\tan\beta$. The couplings of the A to the charged leptons and the down-type quarks are enhanced by a factor of $\tan\beta$, while the coupling to neutrinos and up-type quarks are suppressed by a similar factor. At large values of $\tan\beta$, two of the three neutral bosons have approximately the same mass and the couplings are thus effectively degenerate. This contributes an additional factor of two enhancement in the cross section, $2 \times \tan^2\beta$. Results are presented on the search for a neutral MSSM Higgs boson produced in association with one or more b quarks, as shown in Fig. 1.

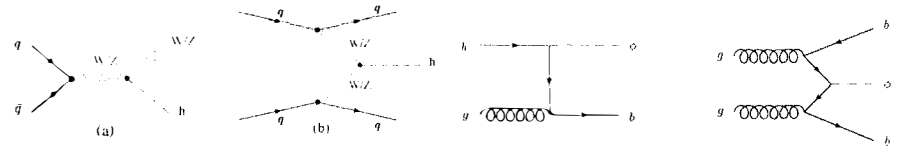

Figure 1: The dominant production diagrams for the benchmark fermiophobic Higgs boson model: associated production with a vector boson (a), and vector boson fusion (b). Neutral scalar production in association with b quarks (the two diagrams on the right).

2 Fermiophobic Analyses

2.1 D0 Analysis

At D0[5,6], events are selected with at least two photon candidates with $|\eta| < 1.1$ and transverse momentum $p_T > 25$ GeV. In addition to the basic photon selection outlined above, a Neural Network (NN) is used to further discriminate jet backgrounds from prompt photons. This NN discriminant is trained using photon and jet Monte Carlo (MC) samples and constructed from well-understood detector variables sensitive to differences between photons and jets. The output of this discriminant (O_{NN}) is shown in Fig. 2 (left). A cut of 0.1 is applied which retains more than 98% of true photons and rejects 40% of misidentified jets. The difference in azimuthal angle of the two photons is also required to be greater than 0.5, which keeps 99% of the Higgs boson signal but reduces prompt QCD photons originating from fragmentation. For each data event that passes the full selection, a 4-component vector is constructed (ω_{pp}, ω_{pf}, ω_{fp}, ω_{ff}) where the value of one element is 1 and other elements are 0 based on whether one or both photon candidates pass a stronger requirement of $O_{NN} > 0.75$. The weight ω_{pp} (ω_{ff}) then represents events where both photon candidates pass (fail) and ω_{pf} (ω_{fp}) represents events where only the leading (subleading) photon candidate passes. The efficiency of this cut for the photon and jet

samples are parametrized as a function of η and used to construct a 4×4 efficiency matrix E. The estimated background composition is 53% from direct diphoton production, 44% from $\gamma j + jj$, and 3% from Drell-Yan. Further sensitivity is gained at D0 by using several variables with a multivariate technique. In addition to the diphoton mass $M_{\gamma\gamma}$, four other variables with kinematic differences between the signal and background are also considered for this analysis: the transverse momentum of the diphoton system $p_T^{\gamma\gamma}$, $\Delta\phi_{\gamma\gamma}$, and the transverse momenta of the leading and subleading photon, p_T^1 and p_T^2, respectively. These well modeled kinematic variables are used to construct a single discriminant from a boosted decision tree (BDT), trained to distinguish a Higgs boson signal from the backgrounds as shown in Fig. 2 (center).

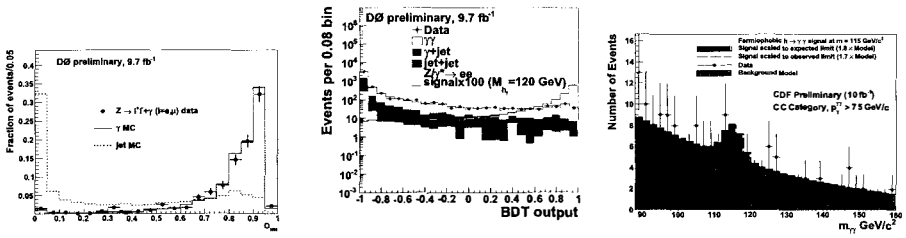

Figure 2: (Left) Neural net output response for photon candidates from diphoton MC, jet MC, and radiative Z boson decays in the data. (Center) The BDT output distributions for a fermiophobic Higgs boson mass of 120 GeV/c^2. (Right) Invariant mass distribution over whole mass range, with an example theoretical Higgs mass at 115 GeV/c^2, scaled to the expected and observed limits obtained from the respective channel alone.

2.2 CDF Analysis

At CDF [7,8], the leading two photons are required to have $p_T > 15$ GeV. Plug photons ($1.2 < |\eta| 2.8$) are selected using a standard photon ID used at CDF. Central photons ($|\eta| < 1.05$) are identified using a NN output constructed from variables sensitive to distinguishing prompt photons from jet backgrounds. This NN discriminant increases the photon signal efficiency by 5% and background rejection by 12% relative to standard photon ID at CDF. The $H \rightarrow \gamma\gamma$ signal acceptance is further increased by reconstructing events in which a single central photon converts into an electron-positron pair, which is found to occur approximately 15% of the time for $|\eta| < 1.05$. A base set of selection requirements is applied that searches for a central electron with a colinear, oppositely signed track nearby. Data events in the CDF analysis are divided into four independent categories according the position and type of the photon candidate. In CC events (the most sensitive category), there are two photons in the central region of the detector. In CP events, one photon is in the central region and one is the plug region. If a CC or CP event is not identified, then two additional categories are considered. In C′C events, both photons are central but one has converted and is reconstructed from its e^+e^- decay products. Finally, in C′P events, one photon is in the plug region and the other is a central conversion photon. For the fermiophobic model, the Higgs boson is typically produced in association with either a W or Z boson or two jets from the VBF process. As a result, the fermiophobic Higgs boson has a higher than average p_T relative to the background processes, as it is typically recoiling against another object. Therefore, the data are further divided into three regions of p_T, where the highest p_T region provides the greatest H_f sensitivity, retaining about 30% of the signal and removing 99.5% of the background. By including the two lower p_T regions, a gain in H_f sensitivity of about 15% is achieved. At CDF, we use a data-driven background model which takes advantage of the Higgs boson mass resolution (3 GeV or less) and smoothly falling background in the signal region of the $M_{\gamma\gamma}$, as shown in Fig. 2 (right). Fits are made to the data excluding a

12 GeV window centered around each Higgs mass hypothesis and for each category. The fit is interpolated into the signal region to determine the background estimation.

3 MSSM Analyses

3.1 D0 Analysis

Two semi-exclusive searches for Higgs boson in association with a b quark are combined: $bh \rightarrow b\tau\tau$ ($\tau_\mu\tau_{had}$) and $bh \rightarrow bb\bar{b}$ using, respectively, 7.3 fb^{-1} and 5.2 fb^{-1} of integrated luminosity [9]. For the $bh \rightarrow b\tau\tau$ ($\tau_\mu\tau_{had}$) channel, data are collected using a mixture of single muon, jet, tau, muon plus jet, and muon plus tau triggers. The efficiency of this selection with respect to the single muon trigger alone is estimated using a sample of $Z \rightarrow \tau_\mu\tau_{had}$ events and found to lie between 80% and 95%. Events are required to contain one isolated muon with a matching central track satisfying $p_T > 15$ GeV and $|\eta_{det}| < 1.6$, and events with more than one muon are rejected to suppress backgrounds from $Z \rightarrow \mu\mu$. Hadronic τ candidates are required to be isolated with $p_T > 10$ GeV and $|\eta| < 2.5$ and selected with a cut on the output of the NN discriminant with an efficiency of around 65% whilst rejecting approximately 99% of hadronic jets. Events must have at least one good b-tagged jet isolated from the muon and tau with $p_T > 15$ GeV, $|\eta| < 2.5$, and $|\eta_{det}| < 2.5$. A cut is placed on the NN_{btag} with an efficiency of around 65% for b quark jets and a 5% fake rate for light quark and gluon jets. Additional rejection of multi-jet and top pair production backgrounds is achieved using a multivariate discriminant, D_{MJ}, and a neural network, $D_{t\bar{t}}$, respectively, both making use of kinematic variables. The distribution of a likelihood discriminant, D_f (Fig. 3), is used as input to the statistical analysis. This is constructed from the various multivariate discriminants, D_{MJ}, D_{tt}, and NN_{btag}. Dominant backgrounds arise from multi-jet production, top pair production, and $Z \rightarrow \tau\tau$ produced with heavy flavor jets.

For the $bh \rightarrow bb\bar{b}$ channel, dedicated triggers are designed to select events with at least three

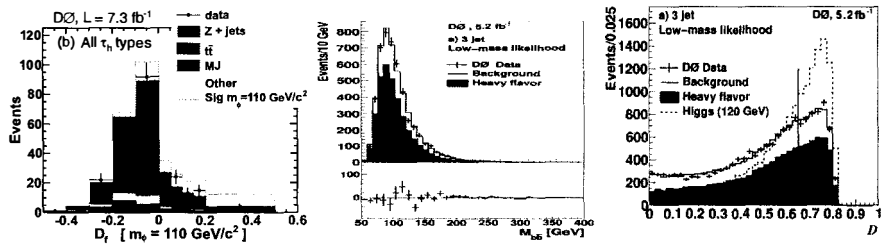

Figure 3: (left) Input distributions for the $bh \rightarrow b\tau\tau$ channels. The final likelihood discriminant distribution summed over all tau types is shown for a Higgs mass of 110 GeV. (center) The dijet invariant mass distribution for the dominant $bh \rightarrow bb\bar{b}$ 3-jet channel is shown. (right) The final discriminant output distributions for an MSSM Higgs boson mass of 120 GeV/c^2.

jets for this analysis. These are approximately 60% efficient for signal with $m_A = 150$ GeV when measured with respect to events with 3 or 4 reconstructed jets. At least three jets within the fiducial region ($p_T > 20$ GeV, $\eta < 2.5$) are required to pass tight NN b-tagging cuts. The per b jet tagging efficiency is around 50% with a light-jet fake rate at the level of 0.5–1.5%. Additionally, the two leading jets must have $p_T > 25$ GeV. Signal sensitivity is further enhanced by breaking the sample into two channels containing exactly 3 or 4 fiducial jets in the final state. A likelihood technique using a set of kinematic variables is employed to further enhance the selection of signal over background. Heavy flavor multi-jet backgrounds dominate and are

estimated using a data-driven method. The binned invariant mass (Fig. 3) distribution of the jet pairing in each event with the highest likelihood value is used in the statistical analysis.

3.2 CDF Analysis

The search is for resonance decays into $b\bar{b}$ [10] in events containing at least three b jet candidates identified by displaced vertices. As the jets resulting from the resonance decay are usually the most energetic jets in the event, the invariant mass of the two leading jets in E_T, denoted m_{12} (Fig. 4), is studied. A signal would appear as an enhancement in the m_{12} spectrum (Fig. 4). The background is predominantly QCD multijet production containing multiple bottom or charm quarks. Events with single pairs of heavy flavor also enter the sample when a third jet from a light quark or gluon is mistakenly tagged. No precise a priori knowledge of the background composition and kinematics is available, and there is no plan to rely upon a Monte Carlo generator to reproduce it well. Instead, a technique is developed to model the m_{12} spectrum

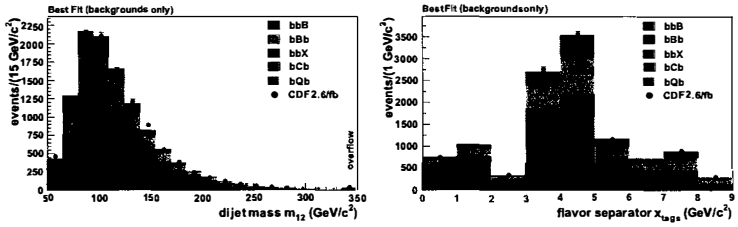

Figure 4: Fit of the triple-tagged data sample using only the QCD background templates, in the m_{12} (Left) and x_{tags} projections (Right).

for the background in the triple-tagged sample in a data-driven manner, starting from double-tagged events. To enhance the separation between the flavor dependent background components and the possible resonance signal, a second quantity x_{tags} is introduced, constructed from the invariant masses of the charged particle tracks forming the displaced vertices, which is sensitive to the flavor composition: three bottom quark jets vs. two bottom quarks and one charm quark, etc. The kinematic information in m_{12} is then complemented by flavor information in x_{tags}.

4 Results

Analyses for the D0 and CDF experiments were discussed which searched for a fermiophobic Higgs boson in the diphoton final state using the full Tevatron dataset. No obvious evidence of a signal is observed and lower limits from D0 and CDF were set on the fermiophobic Higgs boson mass of 111.4 (114) GeV/c^2 at 95% C.L., respectively as shown in Fig. 5. Using up to 8.2 fb^{-1} of data, a Tevatron combination excludes the fermiphobic Higgs boson with masses below 119 GeV/c^2 as shown in Fig. 5. Moreover, D0 and CDF have searched for an MSSM Higgs and the current results exclude a substantial region of the MSSM parameter space, especially for $M_A < 180$ GeV/c^2 and $tan\beta > 20$–30 as shown in Fig. 6. A deviation greater than 2σ is observed by D0 and CDF around 120 GeV/c^2 and 150 GeV/c^2, respectively. However, the statistical significance of this discrepancy is reduced to 2σ or less after the trial factor.

5 Conclusion

Analyses for the D0 and CDF experiments were discussed which searched of evidence for the BEH boson in BSM scenarios, particularly in supersymmetric models and fermiophobic scenarios

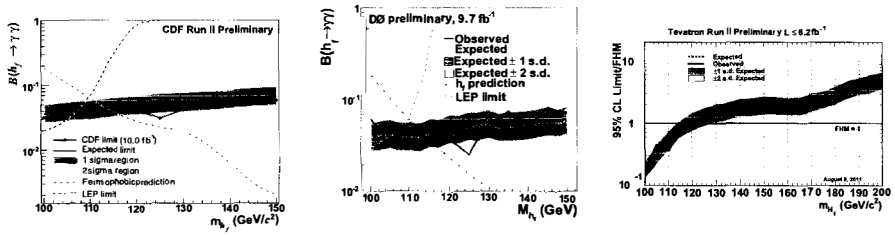

Figure 5: Observed and expected 95% C.L. upper limits on fermiophobic $B(H_f \to \gamma\gamma)$ as a function of the fermiophobic Higgs boson mass for CDF (Left) and D0 (Center). (Right) Tevatron combination (Summer 2011).

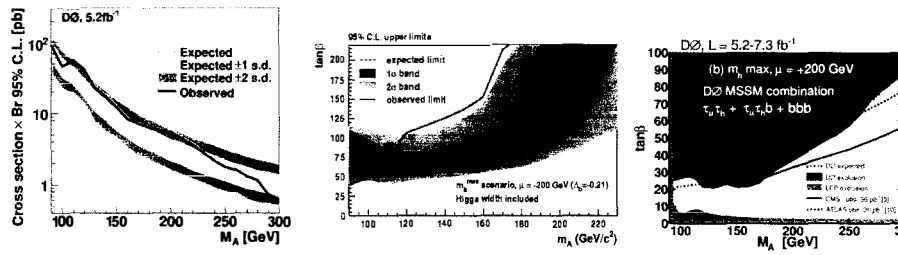

Figure 6: (Left) Limits on $\sigma \times BR$ on MSSM Higgs in the b final states. Constraints in the $(\tan\beta, M_A)$ plane for different MSSM scenarios of CDF result (Center) and a combination of the D0 results discussed above (Right).

using the full Tevatron dataset. No evidence of a signal is observed and hence limits were set.

Acknowledgments

I would like to thank the Fermilab staff, the technical staffs of the participating institutions, and the funding agencies for their vital contributions.

References

1. P.W. Higgs, Phys. Rev. Lett. 13, 508 (1964); G.S.Guralnik, C. R. Hagen, and T.W. B. Kibble, ibid. 13, 585 (1964); F. Englert and R. Brout, ibid. 13, 321 (1964).
2. A.G. Akeroyd, Phys. Lett. B 368, 89 (1996).
3. H. Nilles, Phys. Rep. 110, 1 (1984); H. Haber and G. Kane, Phys. Rep. 117, 75 (1985).
4. A. Rosca (LEP Collaborations), Nucl. Phys. B, Proc. Suppl. 117, 743 (2003)
5. V.M. Abazov et al. (D0 Collaboration), Nucl. Instr. Meth. A 565, 463 (2006).
6. V. M. Abazov et al. (D0 Collaboration), Phys. Rev. Lett. 107, 151801 (2011).
7. F. Abe et al. (CDF), Nucl. Instr. Meth. A 271, 387 (1988).
8. T. Aaltonen et al. (CDF Collaboration), Phys. Rev. Lett. 108, 011801 (2012).
9. V. M. Abazov et al. (D0 Collaboration), Phys. Rev. Lett. 107, 121801 (2011).
10. T. Aaltonen et al. (CDF Collaboration), Phys. Rev. D 85, 032005 (2012).